Journal of Virology

Virology | Full-Length Text

LINC08148 promotes the caveola-mediated endocytosis of Zika virus through upregulating transcription of Src

Zhiting Huo,[1,2] Xuanfeng Zhu,[1,2] Qinyu Peng,[1,2] Cancan Chen,[3] Xiaoyi Yang,[1,2] Changbai Huang,[1,2] Yincheng Xiang,[1,2] Qingju Tian,[1,2] Jingyu Liu,[4] Chao Liu,[1,2] Ping Zhang[1,2]

AUTHOR AFFILIATIONS See affiliation list on p. 16.

ABSTRACT Long non-coding RNAs (lncRNAs) represent a new group of host factors involved in viral infection. Current study identified an intergenic lncRNA, LINC08148, as a proviral factor of Zika virus (ZIKV) and Dengue virus 2 (DENV2). Knockout (KO) or silencing of LINC08148 decreases the replication of ZIKV and DENV2. LINC08148 mainly acts at the endocytosis step of ZIKV but at a later stage of DENV2. RNA-seq analysis reveals that LINC08148 knockout downregulates the transcription levels of five endocytosis-related genes including *AP2B1*, *CHMP4C*, *DNM1*, *FCHO1*, and *Src*. Among them, loss of Src significantly decreases the uptake of ZIKV. *Trans*-complementation of Src in the LINC08148^{KO} cells largely restores the caveola-mediated endocytosis of ZIKV, indicating that the proviral effect of LINC08148 is exerted through Src. Finally, LINC08148 upregulates the *Src* transcription through associating with its transcription factor SP1. This work establishes an essential role of LINC08148 in the ZIKV entry, underscoring a significance of lncRNAs in the viral infection.

IMPORTANCE Long non-coding RNAs (lncRNAs), like proteins, participate in viral infection. However, functions of most lncRNAs remain unknown. In this study, we performed a functional screen based on microarray data and identified a new proviral lncRNA, LINC08148. Then, we uncovered that LINC08148 is involved in the caveola-mediated endocytosis of ZIKV, rather than the classical clathrin-mediated endocytosis. Mechanistically, LINC08148 upregulates the transcription of Src, an initiator of caveola-mediated endocytosis, through binding to its transcription factor SP1. This study identifies a new lncRNA involved in the ZIKV infection, suggesting lncRNAs and cellular proteins are closely linked and cooperate to regulate viral infection.

KEYWORDS long non-coding RNA, Zika virus, host factor, endocytosis, infection

Zika virus (ZIKV) is an emerging arbovirus belonging to *Flaviviridae* family and *Flavivirus* genus (1, 2). ZIKV is primarily transmitted by mosquitoes, also by blood transfusion, sexual contact, and vertical transmission (3, 4). ZIKV infections are normally asymptomatic and self-limiting, while its association with neurological complications including fetal microcephaly and adult Guillain-Barré syndrome raises a global concern (3, 5, 6). To date, ZIKV can still be detected in field-caught mosquitoes worldwide (7–9), posing a potential threat to public health. Nonetheless, no specific drugs are available to treat ZIKV diseases.

ZIKV infection begins with viral envelope protein (E) binding to cellular receptors, followed by internalization through clathrin- or caveola-mediated endocytosis (10). The clathrin-mediated endocytosis involves more than 50 proteins, transporting virions from the plasma membrane into the cell (11). ZIKV employs the clathrin-mediated endocytosis to enter a variety of cells, such as human glioma cell line (SNB19) (12), human cervical carcinoma cells (HeLa) (13), and Vero cells (14). It can also utilize the caveola-mediated

Editor Shan-Lu Liu, The Ohio State University, Columbus, Ohio, USA

Address correspondence to Ping Zhang, zhangp36@mail.sysu.edu.cn, or Chao Liu, liuchao9@mail.sysu.edu.cn.

Zhiting Huo and Xuanfeng Zhu contributed equally to this article. The order of authorship corresponds to the chronological order in which the authors were involved in the project.

The authors declare no conflict of interest.

See the funding table on p. 16.

Received 7 November 2023
Accepted 15 April 2024
Published 14 May 2024

endocytosis to access glioblastoma T98G cells (15). In the low PH environment of endosomes, ZIKV fuses with the endosomal membrane to release viral genomic RNA. The viral RNA encodes a polyprotein, which is cleaved into 10 individual proteins by host and viral proteases, followed by viral RNA replication, protein translation, packaging, and egress (16).

So far, a variety of host proteins have been identified to participate in the replication and transmission of ZIKV (17–20). In contrast, the role of long non-coding RNAs (lncRNAs) in the ZIKV infection remains largely unknown. LncRNAs are non-coding RNAs with a length of more than 200 nucleotides (21). Based on their genomic location, lncRNAs are divided into five types: intergenic, intronic, bidirectional, sense, and antisense lncRNAs (21). LncRNAs are normally expressed at lower levels than proteins and display a tissue- and species-specific expression pattern (22). LncRNAs play a role in various physiological and pathological processes, including development, proliferation, transcription, post-transcriptional modification, apoptosis, and cellular metabolism (23–26). Upon viral infection, cellular lncRNA profiling is often altered, which either shapes cellular responses or influences replication of viruses (27–29). For example, the expression of lncRNA lnczc3h7a is induced by vesicular stomatitis virus (VSV) infection, and it plays an antiviral role through binding to TRIM25 and RIG-I and stabilizing their complex, thereby promoting type I IFN production (30).

Previously, alteration of lncRNAs expression by ZIKV infection has been reported in human neural progenitor cells (hNPCs) (31), *Aedes albopictus* cells (C6/36) (32), and A549 cells (33). Our group reported that in A549 cells, 79 lncRNAs were differentially expressed upon ZIKV infection, and an IFN-inducible lncRNA (OASL-IT1) plays a positive-feedback role in the innate immune response (33). In this study, we identified an intergenic lncRNA (LINC08148) as a proviral factor. We determined that LINC08148 acts at the entry step of ZIKV, and investigated the transcriptional profiling modulated by LINC08148 by RNA-seq. Then, we analyzed the role of five genes regulated by LINC08148 in the viral entry, and uncovered that Src participates in the caveola-mediated internalization of ZIKV into A549 cell. Last, we found that LINC08148 binds to transcription factor SP1 and promotes the transcription of *Src*. This work identified a new lncRNA involved in the ZIKV infection.

RESULTS

Identification and characterization of lncRNAs regulated by ZIKV infection

To identify new lncRNAs involved in the ZIKV infection, we selected nine differentially expressed intergenic lncRNAs (>2-fold change) in the ZIKV-infected cells from lncRNA microarray data (GSE124094) (Fig. S1A). Their levels in the mock- and ZIKV-infected A549 cells were validated by quantitative real-time PCR (qRT-PCR) (Fig. S1B). Among the nine selected lncRNAs, the basal levels of lnc-DGCR6-2:33 and ENST00000608148 were abundant in the mock-infected cells, and their expression was significantly upregulated by ZIKV infection (Fig. 1A; Fig. S1B). According to the HUGO Gene Nomenclature Committee decision tree (34), Lnc-DGCR6-2:33 and ENST00000608148 were designated as LINC-DGCR6 and LINC08148, respectively. To examine the role of these two lncRNAs in the ZIKV infection, we generated gene knockout (KO) bulk cells using CRISPR/Cas9 strategy. Then, control and lncRNA KO cells were infected with ZIKV, and at 24 h postinfection (p.i.), supernatants were harvested for plaque assay. LINC008148 confers a higher proviral activity than LINC-DGCR6 (Fig. 1B and C), so it was chosen for further characterization.

Human LINC08148 is an intergenic lncRNA located on chromosome 10 from position 33,341,655 to 33,341,905. Full-length transcript of LINC08148 is 251 nt, as evidenced by rapid amplification of cDNA ends (RACE) assay (Fig. 1D). Human LINC08148 shares 93.6% homology with rhesus and 88.3% homology with dog, but no homologous gene was identified in mouse and chicken (USCS genome browser, hg38, Fig. S1C), suggesting that LINC08148 is species specific. Coding-Potential Assessment Tool (CPAT) and Phylogenetic Conservation Score of a sORF (PhyloCSF) analysis predicted that LINC08148 possesses an extremely low protein-coding potential as annotated lncRNAs (NEAT1 and Lsm3b) (Fig.

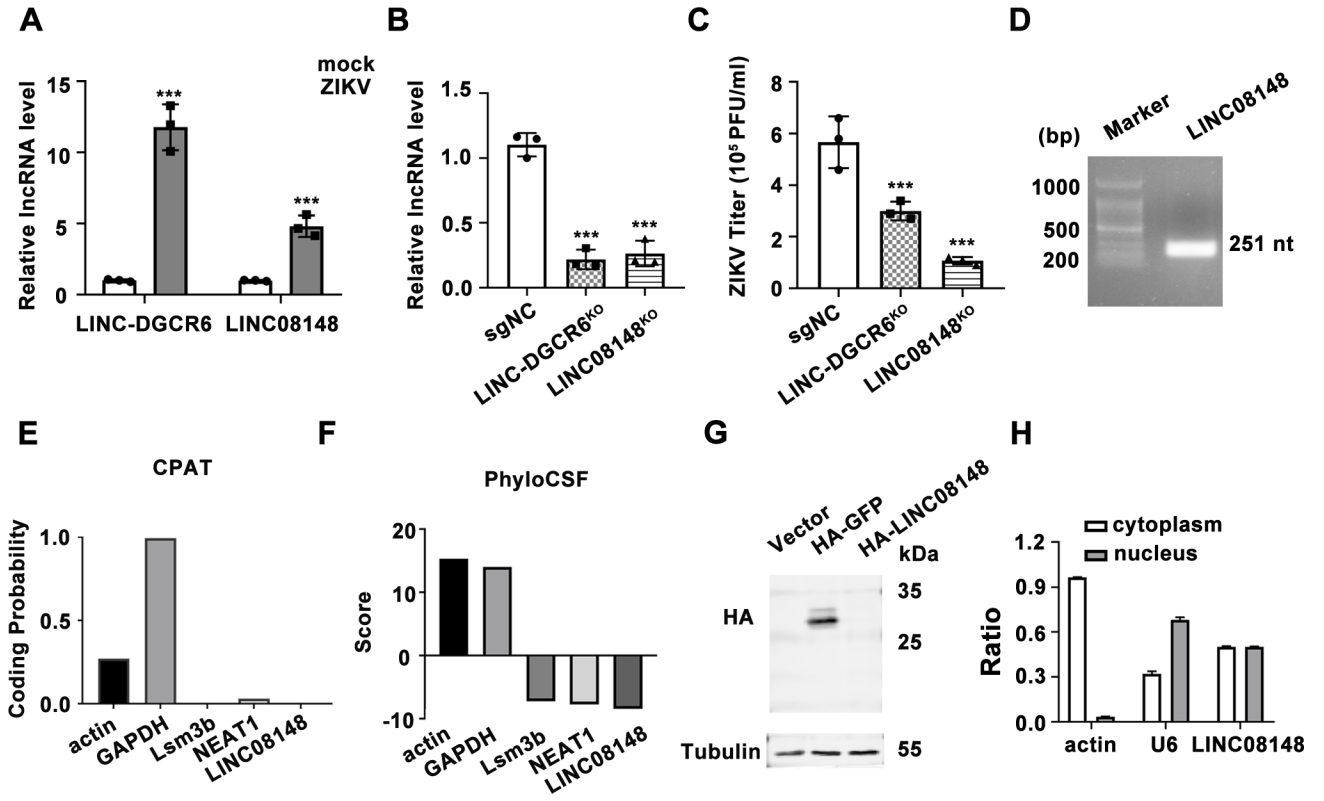

FIG 1 Screen of lncRNAs regulated by ZIKV. (A) Validation of microarray data. A549 cells were infected with ZIKV (multiplicity of infection, MOI 8). At 24 h p.i., the cells were harvested for qRT-PCR to detect the levels of LINC-DGCR6 and ENST08148. β-actin was measured as an internal control. (B, C) Role of two selected lncRNAs in the ZIKV replication. sgNC (negative control sgRNA with scramble sequence), LINC08148, or LINC-DGCR6 KO cells were infected with ZIKV (MOI 1). At 24 h p.i., the cells and supernatants were collected for qRT-PCR to detect the levels of lncRNA (B) or plaque assay (C). GAPDH was set as an internal control. (D–H) Characterization of LINC08148. Size of *LINC08148* was determined by RACE (D). Coding probability of LINC08148 was predicated by PhyloCSF (E) and CPAT (F). β-actin and GAPDH served as coding controls, and Lsm3b and NEAT1 served as non-coding controls. 293T cells were transfected with pcDNA3.1, pcDNA3.1-HA-LINC08148, or pcDNA3.1-HA-GFP. At 24 h post transfection, the cells were harvested for Western blot using anti-HA antibody. Blots were representative of at least three independent experiments (G). (H) Localization of LINC08148. A549 cells were harvested for subcellular fractionation. qRT-PCR was performed to measure the levels of LINC08148, U6, and actin in the cytoplasm and nucleus, respectively. Data are shown as mean ± SD of at least three independent experiments. ***$P < 0.001$, unpaired, two-tailed Student's *t*-test.

1E and F). To validate this prediction, we constructed a eukaryotic vector carrying LINC08148 gene tagged with HA at its N-terminus (pcDNA3.1-HA-LINC08148). 293T cells were transfected with pcDNA3.1-HA-LINC08148 and were harvested for Western blot. No specific band was detected, demonstrating that LINC08148 does not encode protein (Fig. 1G). Subcellular fraction assay data showed that LINC08148 was distributed in both nucleus and cytoplasm (Fig. 1H).

LINC08148 promotes the infection of ZIKV and DENV2

To validate the role of LINC08148 in the flavivirus infection, we generated two LINC08148 knockout A549 cell clones (LINC08148^{KO}) and knockdown bulk A549 cells (LINC08148^{KD}) through CRISPR/Cas9 and RNAi strategies, respectively (Fig. 2A). qRT-PCR data validated that LINC08148 levels in the LINC08148^{KO} and LINC08148^{KD} cells were largely ablated (Fig. 2B and C). Then, control, LINC08148^{KO}, and LINC08148^{KD} cells were infected with ZIKV. At 24 h p.i., the cells and supernatants were harvested for measurement of viral replication levels. In the LINC08148-deficient cells, the ZIKV RNA levels, E protein, and titers were markedly decreased (Fig. 2D through I). Similarly, the replication levels of DENV2 (strain 16681) in the LINC08148^{KO} and LINC08148^{KD} cells, including viral RNA, NS3 protein, and titers, were lower than control cells (Fig. 2J through O). Overall, these results indicated

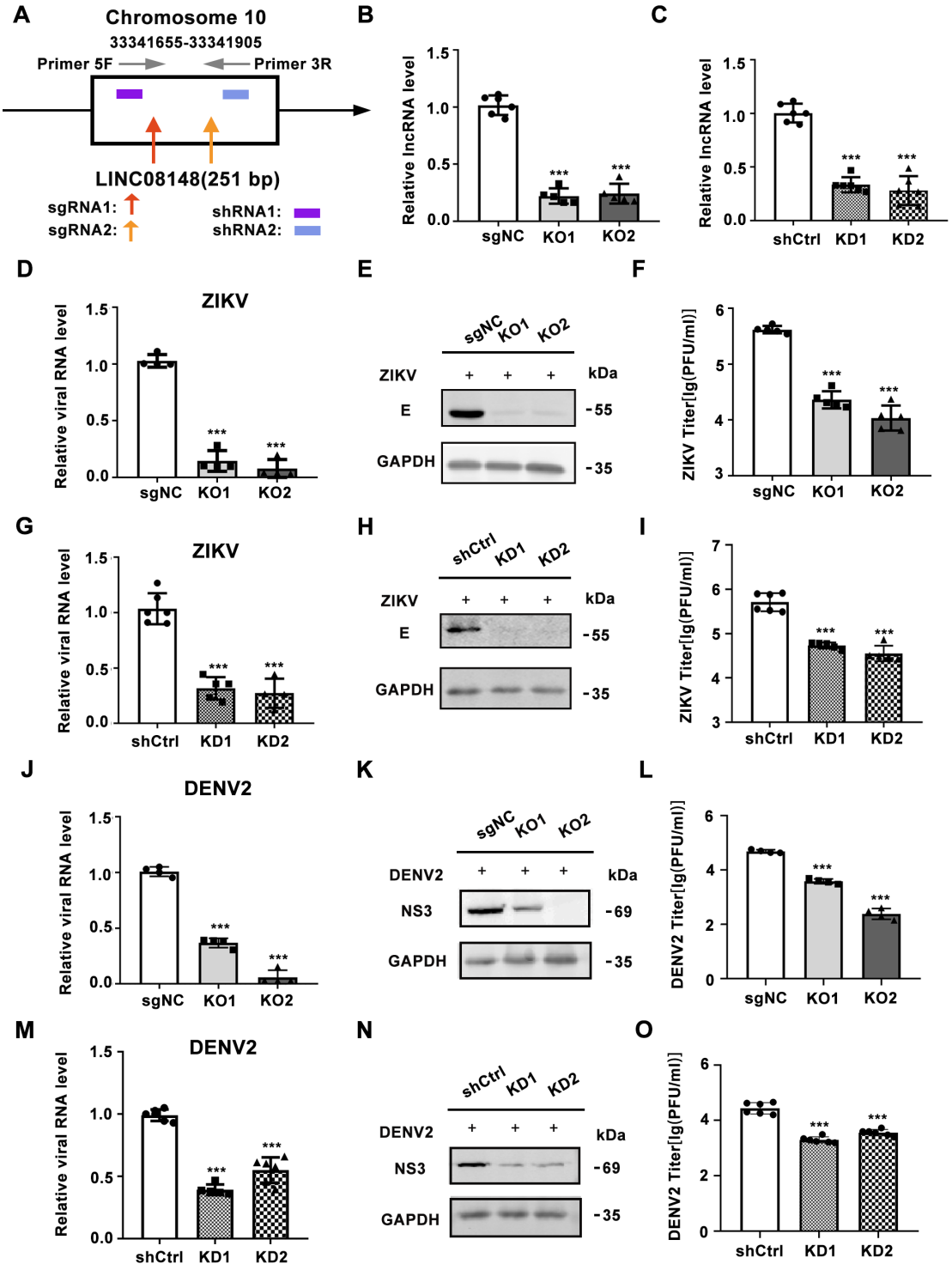

FIG 2 LINC08148 plays a proviral role in A549 cells. (A) Positions of sgRNAs (1 and 2) and shRNAs (1 and 2) against LINC08148, and PCR primers used to amplify *LINC08148*. (B, C) Levels of LINC08148 in A549 cells. sgNC, LINC08148^{KO}, or LINC08148^{KD} cells were harvested for qRT-PCR to measure LINC08148 levels. β-actin served as an internal control. (D–O) Replication levels of ZIKV and DENV2. sgNC and LINC08148^{KO}, or shCtrl (control shRNA with scramble sequence) and LINC08148^{KD} cells were infected with ZIKV (D–I) or DENV2 (J–O). Cells or supernatants were harvested at 24 h p.i. for qRT-PCR to measure the intracellular RNA levels of ZIKV (D, G) or DENV2 (J, M), or for Western blot to detect ZIKV E (E, H) or DENV2 NS3 protein (K, N) levels, or for plaque assay (F, I, L, O). GAPDH served as an internal control. Data are shown as mean ± SD of at least three independent experiments. ***$P < 0.001$, unpaired, two-tailed Student's *t*-test.

that LINC08148 plays a proviral role in the replication of ZIKV and DENV2. Similarly, the LINC08148 knockout led to a significant reduction of Japanese encephalitis virus (JEV) titers in A549 cells (Fig. S2A).

Furthermore, we examined the role of LINC08148 in other cell lines including Huh7 and 293T cells. The data showed that the ZIKV yields in two bulk LINC08148^{KO} Huh7 cells were downregulated by about 10-fold (Fig. S2B). In the bulk LINC08148^{KD} 293T cells, viral replication levels were dramatically reduced (Fig. S2C through F), indicating that the proviral effect of LINC08148 is not cell specific. Intriguingly, although the overexpression of LINC08148 in 293T cells dramatically enhanced the LINC08148 level, the replication levels of ZIKV were not significantly altered (Fig. S2G through J), implying that the endogenous level of LINC08148 might be sufficient for promoting ZIKV replication.

LINC08148 functions at the entry step of ZIKV but not DENV2

To determine which step of viral infection LINC08148 acts at, we compared the kinetic replication levels of ZIKV with the control (negative control sgRNA, sgNC) and LINC08148^{KO} A549 clonal cells at 6, 12, and 24 h p.i. As shown in Figure 3, the RNA and E protein levels of ZIKV in the LINC08148^{KO} cells were significantly lower than in the control cells as early as 6 h p.i. The DENV2 RNA levels in the LINC08148^{KO} cells were comparable to the sgNC cells at 6 and 12 h p.i., and were lower than the sgNC cells at 24 and 36 h p.i. Western blot data showed that at 12 h p.i., a weak band of DENV NS3 was observed in the sgNC cells but not in the LINC08148^{KO} cells; at 24 and 36 h p.i., the NS3 protein levels in two LINC08148^{KO} cells were less abundant than in the sgNC cells (Fig. 3C and D). These results suggested that LINC08148 might act at different steps of ZIKV and DENV2.

Next, we tested the role of LINC08148 in the entry of ZIKV and DENV2. Cells were inoculated with viruses at 4°C for 1 h to allow virions to attach, or at 37°C for 1 h to allow virions to be internalized. Total RNAs were extracted for qRT-PCR to detect the amounts of attached or internalized virions. After 4°C incubation, the RNA levels of ZIKV and DENV2 in the control and LINC08148^{KO} cells were comparable (Fig. 3E and F). In contrast, after 37°C incubation, the RNA levels of ZIKV but not DENV2 were significantly reduced by LINC08148 knockout (Fig. 3E and F). The endocytosis of JEV, another flavivirus member, was also downregulated by LINC08148 depletion (Fig. 3G). To further confirm the role of LINC08148 in the endocytosis of ZIKV and DENV2, we isolated endosome fraction from the mock or virus-inoculated cells, followed by RNA extraction and qRT-PCR. Western blot data showed that early endosome protein EEA1 was present while nuclear Lamin B was absent in the isolated endosome fraction, indicative of successful isolation. The ZIKV RNA levels in the LINC08148^{KO}-derived endosomes were significantly lower than in the control, while the DENV2 RNA levels in the endosomes of control and LINC08148^{KO} cells were comparable (Fig. 3H and I), indicating that LINC08148 specifically regulates the endocytosis of ZIKV.

LINC08148 is involved in the caveolin-1-mediated endocytosis

Considering that nuclear lncRNAs can regulate gene expression in *cis* and *trans* (35), and *NRP1*, a *LINC08148* neighboring gene, mediates the entry of severe acute respiratory syndrome coronavirus 2 (SARS-CoV-2) and Epstein–Barr virus (EBV) (36, 37), we first tested whether LINC08148 affects the ZIKV entry through *cis*-regulating *NRP1* expression. The qRT-PCR data showed that *NRP1* levels in the sgNC and LINC08148^{KO} cells were comparable (Fig. S3A), and *NRP1* silencing had no impact on the ZIKV attachment and endocytosis (Fig. S3B and C), suggesting that LINC08148 function is independent of *NRP1*.

Next, we performed RNA-seq to screen genes regulated by LINC08148 in *trans*. In the LINC08148^{KO} cells, 2,261 genes were upregulated and 1,748 genes were downregulated (adjusted $P < 0.05$). In the Gene Ontology (GO) analysis, the LINC08148 depletion decreases transcription of several genes involved in endocytosis process, such as actin cytoskeleton reorganization and transport vesicles (Fig. S3D). In the Kyoto Encyclopedia of Genes and Genomes (KEGG) pathway analysis, two pathways involved in the virus

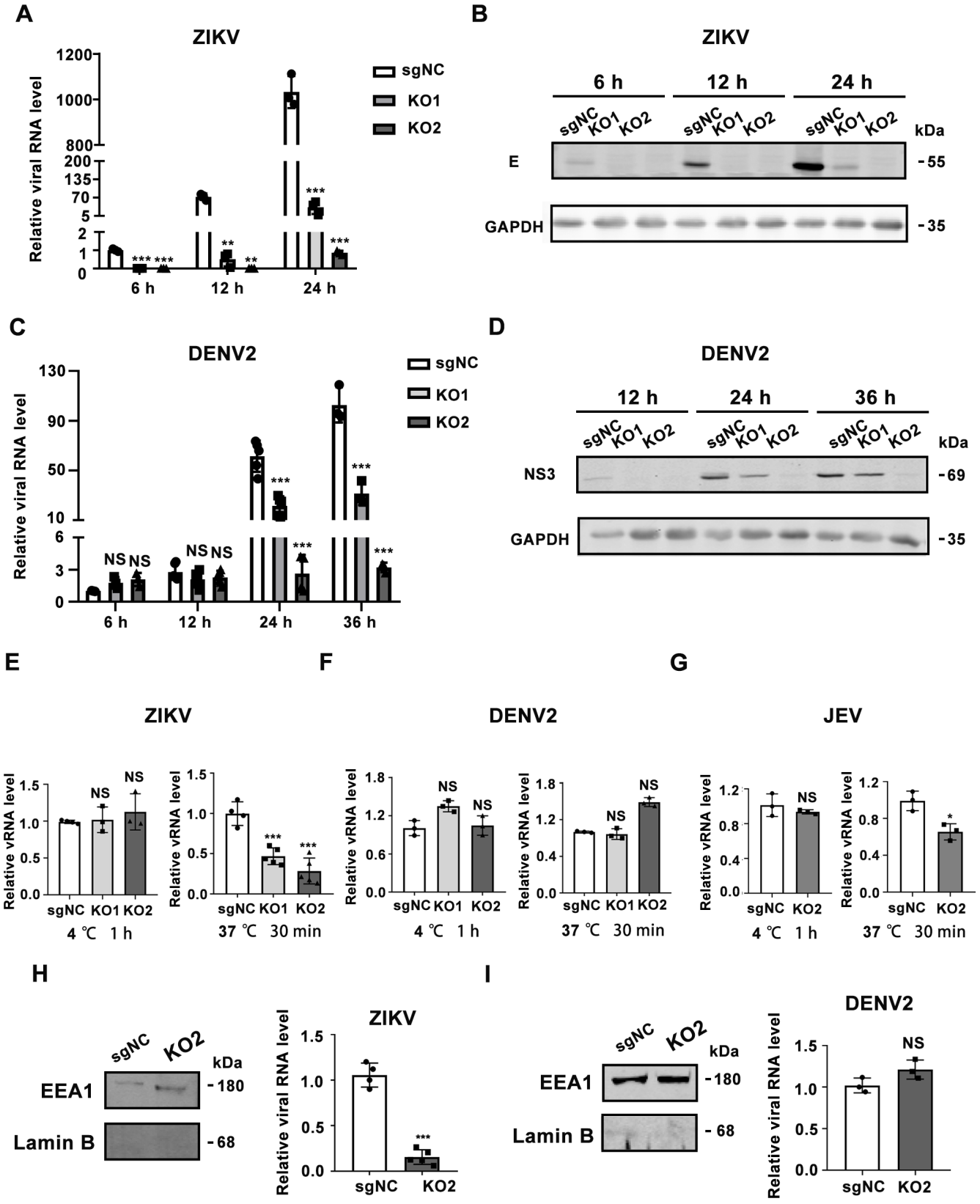

FIG 3 LINC08148 functions at the endocytosis step of ZIKV. (A–D) Kinetic replication levels of viruses. sgNC, LINC08148^{KO1}, and LINC08148^{KO2} cells were infected with ZIKV or DENV2. At indicated time points, the cells were collected for qRT-PCR (A, C) or Western blot using antibodies against ZIKV E, DENV NS3, or GAPDH (B, D). (E–G) Viral entry assay. sgNC and LINC08148^{KO} cells were inoculated with ZIKV (E), DENV2 (F), or JEV (G) at 4°C or 37°C for 30 min. The cells were harvested

(Continued on next page)

FIG 3 (Continued)

for qRT-PCR to measure the levels of attached (E) or internalized virions (F). (H, I) Endosome isolation assay. sgNC and LINC08148^{KO2} cells were infected with ZIKV or DENV2 for 30 min. Endosomes were isolated and applied for Western blot or qRT-PCR. Antibodies against endosome marker EEA1 and nucleus marker Lamin B1 were used as internal control. Viral RNA levels in the endosome were normalized to endosome proteins. Data are shown as mean ± SD of at least three independent experiments. NS, no statistical significance; ***$P < 0.001$, unpaired, two-tailed Student's *t*-test.

endocytosis, namely, lysosome and cell adhesion molecules, were highly enriched (Fig. S3E). To validate the RNA-seq data, we selected 12 genes involved in the flavivirus endocytosis, including *AP2B1*, *CHMP4C*, *CLTC*, *DNM1*, *DNM2*, *FCHO1, LY6E*, *RAB5A*, *RAB7A*, *RAB9A*, *RAB11A*, and *Src* for qRT-PCR measurement (38). Consistent with RNA-seq data, the levels of *AP2B1*, *CHMP4C*, *DNM1*, *FCHO1,* and *Src* were reduced, while *RAB9A* was increased by LINC08148 depletion (Fig. 4A and B). Levels of another seven genes were comparable in the control and LINC08148^{KO} cells (Fig. S3F).

Among the five genes downregulated by LINC08148 depletion, *FCHO1*, *DNM1*, and *AP2B1* are involved in the clathrin-mediated endocytosis (39–41), and *Src* is an initiator of the caveolin-mediated endocytosis (42–44). To determine through which pathway(s) ZIKV and DENV2 enter into A549 cells, we utilized two chemical inhibitors, CPZ (inhibitor of the clathrin-mediated endocytosis) (45, 46) and nystatin (inhibitor of the caveolin-mediated endocytosis) (47, 48). At working concentrations, CPZ (40 µM) and nystatin (80 µM) did not affect the cell viability of A549 (Fig. S4). A549 cells were pretreated with CPZ or nystatin for 1 h, followed by virus infection. The qRT-PCR data showed that ZIKV RNA levels in the CPZ- or nystatin-treated cells were both significantly decreased (Fig. 4C), suggesting that ZIKV enters into A549 cells via both clathrin- and caveolin-mediated endocytosis. In contrast, the RNA levels of DENV2 were only reduced by CPZ but not by nystatin, implying that DENV2 enters A549 cells mainly via the clathrin-dependent endocytosis (Fig. 4C). To be noted, the entry levels of ZIKV in the LINC08148^{KO} cells were not further decreased by nystatin treatment (Fig. 4D), suggesting that LINC08148 regulates the caveolin-mediated endocytosis of ZIKV.

Next, we tested the role of *AP2B1*, *CHMP4C*, *DNM1*, *FCHO1*, or *Src* in the ZIKV entry using shRNA specifically targeting these genes. Knockdown efficiencies of most shRNAs, except *FCHO1,* were more than 50% (Fig. 4E). In the viral entry assay, the endocytosis level of ZIKV was significantly reduced by knockdown of *Src* but not by other genes (Fig. 4F), suggesting that Src plays an essential role in the ZIKV entry.

LINC08148 regulates the ZIKV endocytosis through Src

Considering that LINC08148 promotes *Src* transcription, and Src is the key kinase to phosphorylate caveolin-1 (42, 43), we proposed that the impact of LINC08148 on ZIKV uptake might be dependent on Src. To test this hypothesis, we examined the role of Src in the entry of ZIKV and DENV2 in A549 cells by generating Src stable knockdown (Src^{KD}) or knockout cells (Src^{KO}). Western blot data showed that the protein levels of Src in the Src^{KD} and Src^{KO} cells were markedly reduced (left panels, Fig. 5A and B). The Src depletion significantly decreased the endocytosis of ZIKV but not DENV2 (middle panels, Fig. 5A and B). Consistently, the viral yields of ZIKV in the Src^{KD} and Src^{KO} A549 cells were downregulated (Fig. 5A and B). Interestingly, DENV2 titer was reduced by twofold in the Src^{KD} and Src^{KO} A549 cells, implying Src might participate in a later stage of DENV2 infection. The endosome isolation assay confirmed that the ZIKV RNA levels in the endosomes of Src^{KD} cells were lower than in the control cells (Fig. 5C). Src knockdown in 293T cells also led to significant reduction of the internalization, viral RNA level, and titer of ZIKV (Fig. S5A through D) but not DENV2 (Fig. S5E through H). Furthermore, our data revealed that the levels of ZIKV replication and Src transcription in A549 cells were not affected by LINC08148 overexpression alone (Fig. S5I through L), consistent with the data from 293T cells (Fig. S2G through H).

Next, we examined whether the ZIKV uptake in the Src^{KD} cells was affected by CPZ or nystatin. Blockage of clathrin-pathway by CPZ reduced the ZIKV endocytosis level in both

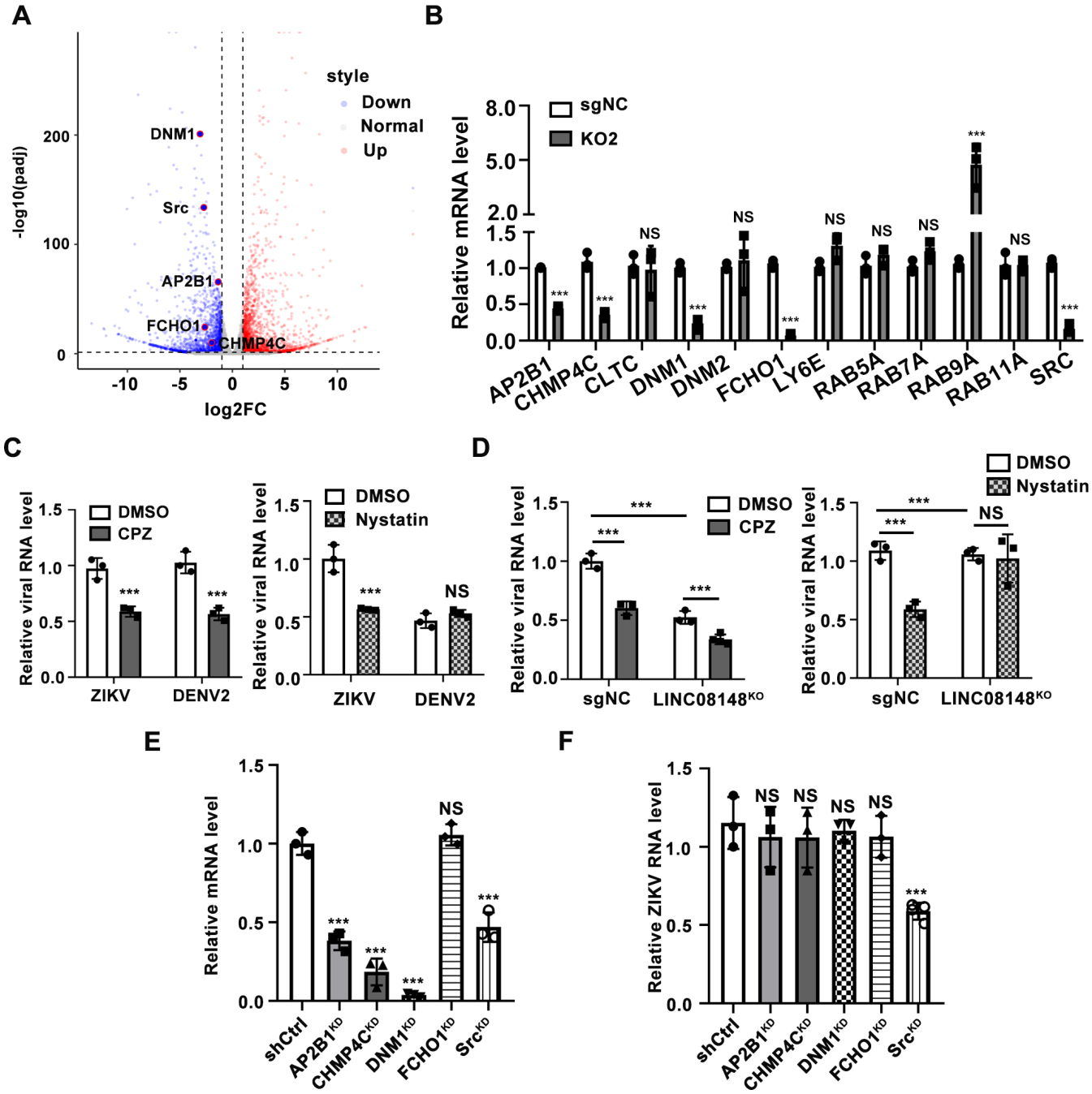

FIG 4 LINC08148 is required for caveolin-1-mediated endocytosis. (A) Volcano plots. Five endocytosis-related and differentially expressed genes in the LINC08148^{KO} cells are highlighted in red. (B) Validation of 12 endocytosis-related genes in the sgNC or LINC08148^{KO} cells by qRT-PCR. (C, D) Inhibitor assay. Cells were pretreated with dimethyl sulfoxide (DMSO), CPZ (40 µM), or nystatin (80 µM) for 1 h, followed by ZIKV inoculation (MOI 3) for 30 min. Cells were harvested for qRT-PCR to detect the RNA levels of internalized virus. (E) Efficiency of shRNA knockdown. A549 cells were transduced with lentiviruses carrying shRNA targeting *AP2B1*, *CHMP4C*, *DNM1*, *FCHO1*, *Src*, or scramble shRNA for 1 h, and were selected with puromycin. Total RNAs were extracted for qRT-PCR assay to measure mRNA levels. (F) Control or shRNA-transfected cells were infected with ZIKV (MOI 3) for 1 h and then harvested for qRT-PCR to detect the RNA levels of internalized virus. β-actin was set as an internal control. Data are shown as mean ± SD of at least three independent experiments. NS, no statistical significance; ***$P < 0.001$, unpaired, two-tailed Student's *t*-test.

the control and Src^{KD} cells (Fig. 5D), while blockage of caveolin-pathway by nystatin did not alter the ZIKV uptake in the Src^{KD} cells (Fig. 5E), suggesting that Src is mainly involved in the caveolin-mediated endocytosis. We further tested the role of Src in the LINC08148-mediated ZIKV endocytosis by *trans*-complementing *Src-FLAG* gene into the LINC08148^{KO}

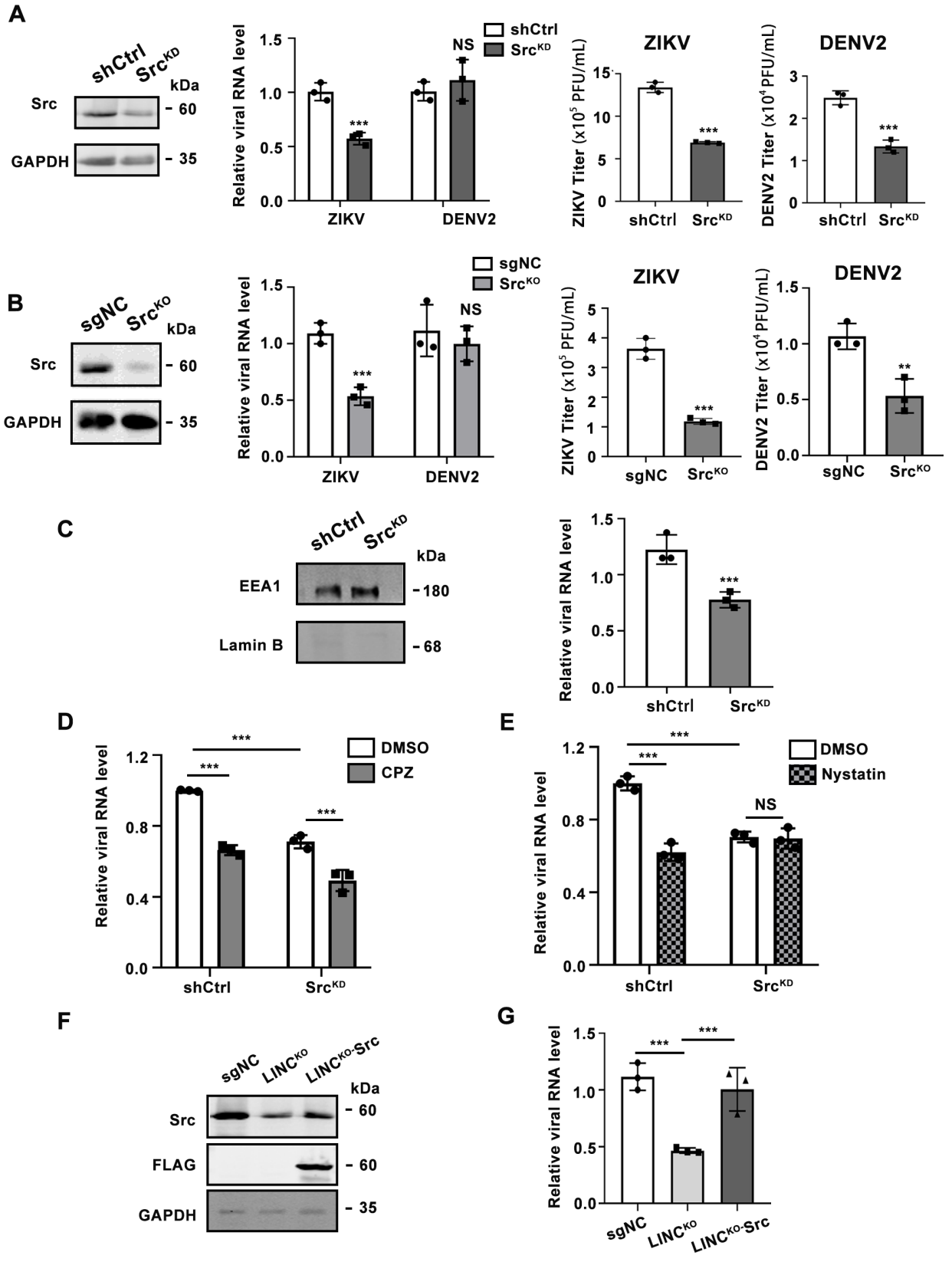

FIG 5 LINC08148 promotes ZIKV endocytosis through Src. (A, B) Role of Src in viral endocytosis and replication. Cells (A: shCtrl and Src^{KD}; B: sgNC and Src^{KO}) were infected with mock, ZIKV, or DENV2 for 30 min (entry) or 24 h (replication). The cells and supernatants were harvested for Western blot, qRT-PCR, and plaque assay. (C) Endosome isolation assay. shCtrl and Src^{KD} cells were infected with ZIKV (MOI 10) for 30 min. Endosomes were isolated for Western blot or qRT-PCR.
(Continued on next page)

FIG 5 (Continued)

Endosomal EAA1 and nucleic Lamin B1 were detected by Western blot. Viral RNA levels in the endosomal fraction were normalized to total endosomal proteins. (D, E) Inhibitor assay. shCtrl and Src^{KD} cells were pretreated with DMSO, CPZ (40 µM) (D), or nystatin (80 µM) (E) for 1 h, followed by inoculation with ZIKV (MOI 3) for 30 min. Viral RNA levels were detected by qRT-PCR. (F, G) *Trans*-complementation of Src restores the viral endocytosis in LINC^{KO} cells. sgNC, LINC08148^{KO}, and LINC^{KO}-Src cells were infected with ZIKV (MOI 3) for 30 min. The cells were harvested for Western blot using antibodies against Src, FLAG, or GAPDH (G), or for qRT-PCR (H). Data are shown as mean ± SD of at least three independent experiments. NS, no statistical significance; ***P < 0.001, unpaired, two-tailed Student's *t*-test.

cells to generate LINC^{KO}-Src cells. The level of Src protein in the LINC^{KO}-Src cells was restored (Fig. 5F), and as expected, the ZIKV uptake level was rescued (Fig. 5G). These collective data illustrated that Src is an essential mediator involved in the LINC08148 function.

LINC08148 regulates the transcription of Src through binding to SP1

To probe how LINC08148 promotes the *Src* transcription, we searched potential transcription factors (TFs) of Src using the online bioinformatics software (_8.3), and we predicted the interaction tendency between these TFs and LINC08148 using catRAPID database. Among them, GR-β and GTF2I possess the highest interaction tendency with LINC08148 (Fig. S6). To test the association between LINC08148 and potential TFs of Src, we constructed vectors expressing GR-β, GTF2I, as well as SP1 and HNF1A, which have been reported TFs of Src (49–51) fused with HA at their C-termini. The 293T cells were transfected with TF-HA-expressing plasmids and were harvested at 24 h for RNA immunoprecipitation (RIP) assay. Western blot data confirmed the all TF proteins were expressed and enriched upon RIP assay. LINC08148 was significantly enriched in the SP1 and GR-β complexes, while HNF1A and GTF21 had low affinity with LINC08148 (Fig. 6A).

To examine the role of SP1 and GR-β in regulating the SP1 transcription, we silenced SP1 by RNAi but overexpressed GR-β in A549 cells, because the endogenous level of SP1 was pretty high while GR-β was extremely low based on the qRT-PCR measurement. Transfection of siRNA against SP1 (siSP1) effectively decreased the levels of SP1 in both the control and LINC08148^{KO} cells (Fig. 6B), and resulted in a significant reduction of Src level in the control cells but not in the LINC08148^{KO} cells, suggesting that SP1 regulates the Src transcription in a LINC08148-dependent manner. The overexpression of GR-β significantly upregulated the *GR-β* mRNA level in A549 cells, but the level of Src was not altered (Fig. 6C), excluding a role of GR-β in the Src transcription. The above data indicated that LINC08148 promotes the Src transcription through SP1.

DISCUSSION

LncRNAs are emerging as a novel group of host factors regulating viral infection. However, a majority of lncRNAs have not been annotated yet. This work identified LINC08148 as a new factor of several *Flaviviridae* members, ZIKV, DENV2, and JEV. Our findings revealed that one of the LINC08148 pro-ZIKV mechanisms is exerted through binding to SP1, hence regulating the transcription of Src, a key initiator of caveolin-mediated endocytosis.

This work focused on intergenic lncRNAs, because loss-of-function strategies could be easily applied without disrupting other genes. Among them, LINC08148 is abundantly expressed and confers a potent proviral activity. Our work demonstrated that LINC08148 does not encode protein and is localized in both nuclei and cytoplasm. The loss-of-function study (including knockout and knockdown strategies) indicated that LINC08148 is a proviral factor of flaviviruses. Interestingly, LINC08148 depletion leads to significant decrease of ZIKV endocytosis and replication at early time, but impairs the replication levels of DENV2 only at its late stage (24 h p.i.). Therefore, we postulate that LINC08148 possesses multiple functions during viral infection. It regulates the entry step of ZIKV but acts at the assembly or egress of DENV2.

By utilizing chemical inhibitors, we demonstrated that ZIKV enters into A549 cells through both clathrin- and caveolin-mediated endocytosis, while DENV2 mainly relies on

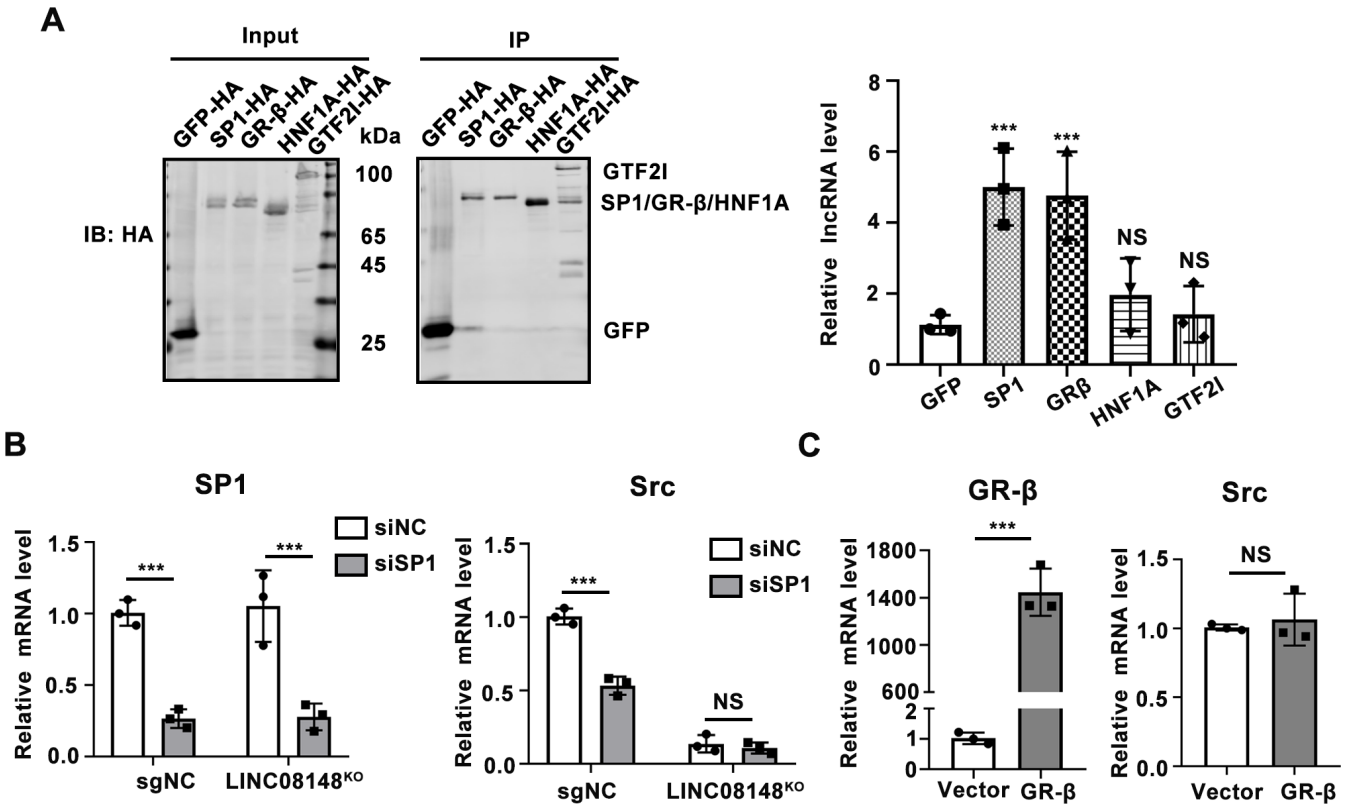

FIG 6 LINC08148 regulates the transcription of Src by interacting with SP1. (A) RIP assay. 293T cells were co-transfected with plasmid expressing LINC08148 and plasmids expressing GFP, SP1, GR-β, HNF-1A, or GTF2I. Whole cell extracts were prepared for RIP assay using HA beads. Total RNAs in the protein–RNA complexes were extracted by TRIzol and detected by qRT-PCR. (B) Role of SP1 in Src transcription. sgNC and LINC08148^{KO} cells were transfected with siNC or siSP1 for 48 h, then harvested for qRT-PCR to detect levels of Src and SP1. (C) Impact of GR-β on *Src* transcription. A549 cells were transfected with vector or plasmid expressing GR-β-HA. At 48 h post-transcription, the cells were harvested for qRT-PCR. Human β-actin was measured as an internal control. Data are shown as mean ± SD of at least three independent experiments. NS, no statistical significance; ***$P < 0.001$, unpaired, two-tailed Student's *t*-test.

clathrin. The observation that nystatin treatment did not further reduce the endocytosis of ZIKV in the LINC08148^{KO} cells illustrated that LINC08148 predominantly regulates the caveolin-mediated endocytosis. ZIKV and DENV, despite their close relationship in evolution, employ different endocytosis pathways. The employment of both caveolin and clathrin by ZIKV might enable it to infect a broader spectrum of tissues.

The RNA-seq profiling data showed that LINC08148 KO leads to alteration of transcription of large amounts of genes, among them several endocytosis-related pathways were highly enriched. Particularly, *AP2B1*, *CHMP4C*, *DNM1*, *FCHO1*, and *Src* were validated to be transcriptionally regulated by LINC08148. In the clathrin-mediated pathway, *FCHO1* and *AP2B1* encode adapters to bind to plasma membrane and recruit proteins, and *DNM1* encodes dynamin required for scission of clathrin-coated pit (39, 40, 52). CHMP4C has been reported to play a role in the envelopment of HSV-1 (53). Nonetheless, the knockdown of *AP2B1*, *CHMP4C*, and *DNM1* alone did not significantly alter the ZIKV entry, suggesting that their functions could be compensated by other paralog proteins such as *DNM2/3* and *AP1B1* (54, 55), or CHMP4C is not employed in the ZIKV invasion. As we failed to effectively silence *FCHO1* even using three different shRNAs, the role of FCHO1 in the entry of ZIKV could not be determined yet. Nonetheless, the depletion of Src successfully reduces the uptake and replication of ZIKV, establishing a role of Src in the entry step of ZIKV. As Src is an initiator of caveolin-mediated endocytosis by phosphorylating caveolin (42, 43), this observation provides further evidence that ZIKV exploits the caveolin-mediated endocytosis to enter into A549 cells, in addition to glioblastoma T98G cells (15).

Importantly, our data revealed that LINC08148 regulates the caveolin-mediated endocytosis of ZIKV, rather than the clathrin-mediated pathway. Ectopic expression of Src can restore the endocytosis level downregulated by LINC08148 loss, illustrating that Src is the key mediator in the LINC08148 proviral effect. Interestingly, although Src knockdown did not directly affect the uptake of DENV2, its loss did slightly impair the viral yield in A549 cells. We proposed that Src might affect a later step of DENV replication, as supported by previous work showing that dasatinib, an Src inhibitor, prevents the assembly and maturation of DENVs (56). To be pointed out, as LINC08148 modulates transcription of genes involved in the actin cytoskeleton reorganization and transport vesicles, it could also modulate the ZIKV uptake through regulating these genes.

Nuclear lncRNAs have been implicated to modulate gene transcription by binding to transcriptional factors, such as lncRNA MALAT1 that interacts with cyclic adenosine monophosphate response element–binding protein (CREB) to regulate stimulator of interferon gene (STING) transcription (57). In this study, LINC08148 also confers an activity to bind to SP1 and to enhance the transcription of Src. As LINC08148 is located in cytoplasm and nuclei, its association with SP1 might take place both outside and inside of nuclei. The lncRNA-TFs association might either facilitate translocation of TFs from cytoplasm to nuclei, or serve as a scaffold for TFs to bind the promoter region of *Src*, thereby promoting the transcription of *Src*. Notably, the overexpression of LINC08148 alone in 293T or A549 cells did not enhance the transcription of Src and ZIKV replication levels, suggesting that either LINC08148 is not sufficient to regulate *Src* transcription by its own and other factors are required (such as SP1), or the endogenous LINC08148 is abundant enough to support viral replication, so LINC08148 overexpression does not show an impact. A detailed mechanism needs to be further investigated.

In summary, our work identified a new lncRNA, LINC08148, which is involved in the infection of several flavivirus members, including ZIKV, DENV2, and JEV, in multiple human cell lines (A549, Huh7, and 293T). Mechanistically, LINC08148 binds to SP1, which facilitates the transcription of Src, a key initiator of caveolin-mediated endocytosis. As ZIKV enters cells through both clathrin- and caveolin-mediated pathways, its entry is partially blocked by LINC08148 or Src depletion. In contrast, the entry of DENV2 that mainly involves clathrin is barely affected by the depletion of either LINC08148 or Src (Fig. 7). Dependency of different entry pathways of flaviviruses might partially contribute to their different tissue tropisms. LINC08148 could be potential therapeutic targets in the treatment of ZIKV diseases.

MATERIALS AND METHODS

Cell culture

Human lung carcinoma epithelial cells (A549, ATCC CCL-185) and human embryonic kidney cells (293T, ATCC CRL-3216) were maintained in Dulbecco's modified Eagle medium (DMEM, Gibco) supplemented with 10% fetal bovine serum (FBS, Gibco) at 37°C with 5% CO_2. African green monkey kidney cells (Vero, ATCC CCL-81) and baby hamster kidney cells (BHK21, ATCC CCL-10) were maintained in DMEM supplemented with 5% FBS at 37°C with 5% CO_2. Mosquito cell line C6/36 (ATCC, CRL-1660) was maintained in RPMI-1640 medium (Invitrogen) supplemented with 10% FBS, 1% sodium pyruvate at 28°C. Media were supplemented with 100 units/mL of streptomycin and penicillin (Invitrogen).

Virus, virus infection, and titration

ZIKV (H/PF/2013 strain, GenBank accession number KJ776791), DENV2 (16681 strain), and JEV (SA14-14-2) were provided by the Guangzhou Centers for Disease Control. ZIKV and DENV2 were amplified in Vero or C6/36 cells. Supernatants were collected when cytopathic effect appeared, and cellular debris was removed by centrifugation. Viral titers were titrated on Vero cells, and viral stocks were stored at −80°C. In a single-step virus growth assay, cells were infected with ZIKV at a multiplicity of infection (MOI) of 1 or JEV

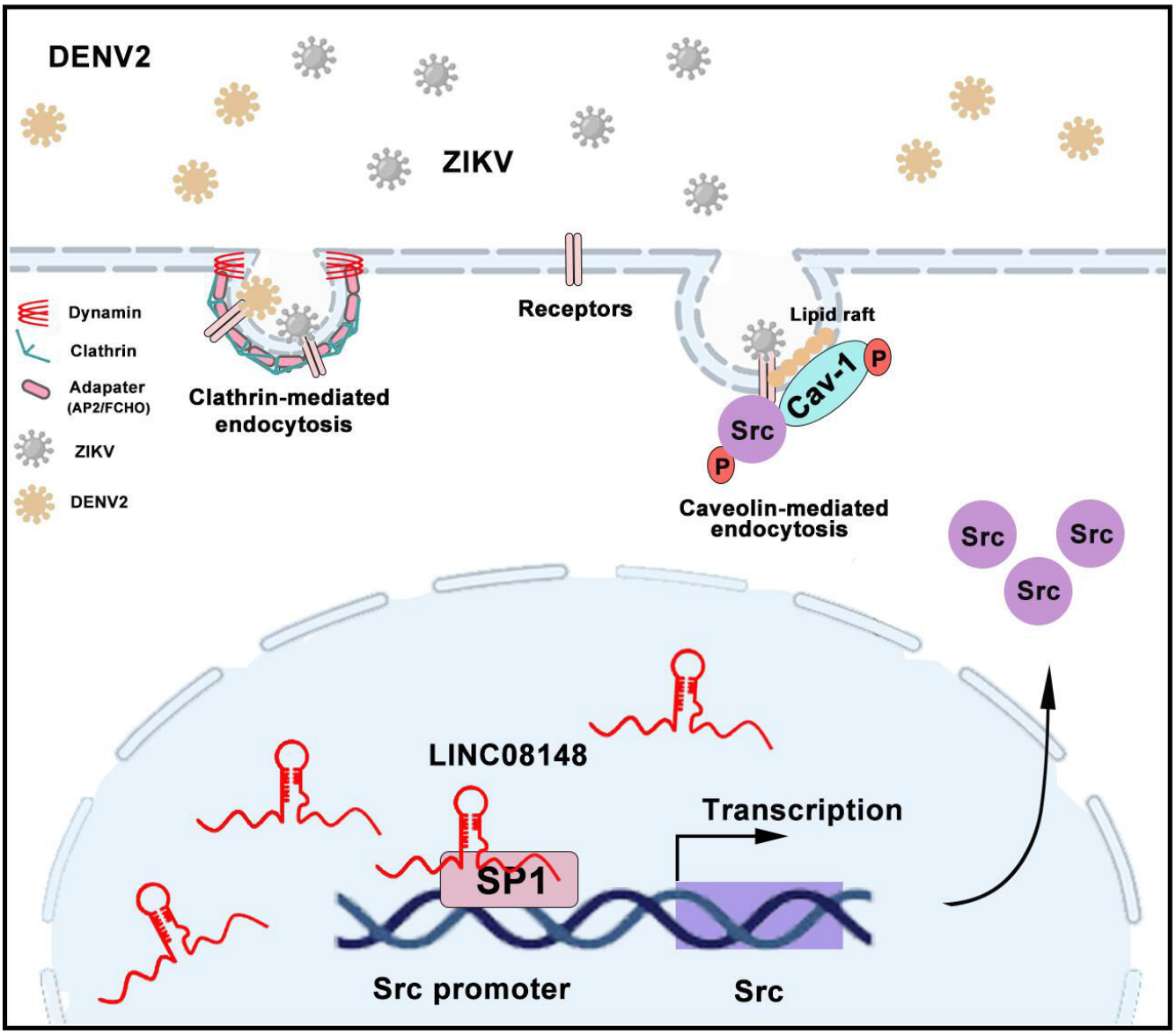

FIG 7 A proposed schematic diagram to illustrate the mechanism of LINC08148 proviral function. LINC08148 binds to transcriptional factor SP1, facilitating its association with the promoter region of *Src* and hence enhancing the transcription of *Src*. Src plays an essential role in the caveolin-1-mediated endocytotic pathway of ZIKV. As DENV2 is mainly internalized through clathrin-mediated pathway, its endocytosis is not regulated by LINC08148.

at an MOI of 3. Supernatants were harvested at 24 h p.i. for virus titration. Virus titers were determined by a standard plaque assay on Vero (ZIKV) or BHK21 (DENV2 and JEV). Serial 10-fold dilutions of each sample were prepared, and 100 µL/well of diluted virus was added into the 24-well plates. Media were removed and cultured in the mixture of two DMEM (Invitrogen) and 2% methylcellulose (Sigma) (1:1). Visible plaques were counted 3–4 d (ZIKV), 5–6 d (DENV2), and 4–5 d (JEV).

Viral entry assay

Cells were incubated with ZIKV or DENV2 at an MOI of 3 at 4°C for 1 h or 37°C for 30 min. Supernatant was removed, and cells were extensively washed three times with cold PBS. Total RNA was extracted using TRIzol (Invitrogen), and viral RNA levels were measured by qRT-PCR.

Endosome isolation

Cells were infected with ZIKV at an MOI of 10 for 0.5 h and then washed twice by PBS. Endosomes were isolated using the Minute Endosome Isolation kit (Invent) according to their instruction. Separated components were resuspended in Buffer RLT (Qiagen) for RNA extraction or RIPA lysis buffer (Beyotime Biotechnology) for immunoblotting. Purity of endosomes was tested using antibodies against endosome-specific protein EEA1 (Cell Signaling Technology) and nucleic Lamin B1 (Cell Signaling Technology).

Plasmid construction

LncRNAs were amplified by 5′- and 3′-RACE PCR using the SMARTer RACE cDNA amplification kit (TaKaRa) and were cloned into the pcDNA3.1(+) vector.

To generate plasmids carrying sgRNAs or shRNAs, a pair of forward and reverse oligonucleotides was annealed and inserted into vectors LentiCRISPR v2 or pLKO.1-TRC (Addgene). Sequences of oligonucleotide used for generation of sgRNAs or shRNAs are listed in Table S2 and S3. Positive plasmids were verified by sequencing and were designated as pLenti-sgLINC08148-1, pLenti-sgLINC08148-2 (targeting *LINC08184*), pLenti-sgLINC-DGCR6-1, pLenti-sgLINC-DGCR6-2 (targeting *LINC-DGCR6*), pLenti-sgSrc-1 (targeting *Src*), and pLenti-sgSrc-2 (targeting *Src*).

Plasmids pEnCMV-Src-3×FLAG (P20814), pEnCMV-SP1-HA-SV40-Neo (P29667), pCMV-FLAG-HNF1A-2-EGFP-SV40-Neo (P37424), pEnCMV-GTF2I-3×FLAG (P18601), and pCDNA3.1-HA-GRβ (P17809) were purchased from http://www.miaolingbio.com/. HNF1A-HA, GTF2I-HA, or Src-3 ×FLAG fragments were amplified by PCR and were cloned into pLVEF1a-IRES-Blast vector. Sequences of PCR primers are listed in Table S4. Positive plasmids were verified by sequencing.

Quantitative real-time PCR

Total RNAs were reversely transcribed using HI Script Q RT SuperMix (Vazyme). cDNAs were used as templates for qRT-PCR using LightCycler 480 SYBR Green I Master (Roche, Basle, Switzerland) on CFX96 Real-Time System (Bio-Rad, Basle, Switzerland). Differences were analyzed using $^{\Delta\Delta}$CT values . Human U6 or β-actin mRNA levels were set as an internal control. Sequences of primer used in qRT-PCR are listed in Table S1.

Western blotting

Cells were lysed with RIPA lysis buffer (pH 7.4) (50 mmol/L Tris-HCl, 150 mmol/L NaCl, 0.5% NP-40, 1% Triton X-100, 1 mmol/L EDTA, 1 mmol/L PMSF, 1% protease inhibitor cocktails, 1 mmol/L Na_3VO4, and 1 mmol/L NaF). Cell extracts were separated on SDS-PAGE and were transferred onto nitrocellulose membranes, followed by blocking in 0.1% PBST with 5% BSA (New England Biolabs) and by incubating with primary antibodies at 4°C overnight. The primary antibodies included anti-glyceraldehyde-3-phosphate dehydrogenase (anti-GAPDH; Proteintech), anti-ZIKV E (GeneTex), anti-Lamin B (Santa Cruz Inc), anti-NS3, anti-HA, anti-FLAG, anti-EEA1, and anti-Src (CST). Detection was performed with IRDye 800 CW-conjugated anti-rabbit IgG and IRDye 680 CW-conjugated anti-mouse IgG secondary antibody (LI-COR) according to the manufacturer's protocols or horseradish peroxidase-conjugated secondary antibodies (Bio-Rad). Immunoreactive bands were visualized using an Odyssey IR imaging system (LI-COR). Western blotting bands were quantified by Quantity One (Bio-Rad).

Establishment of stable knockout, knockdown, or Src overexpressing cells

To generate stable KO, KD, or overexpressing cells, lentiviruses expressing shRNA, sgRNA, LINC08148, or Src were packaged in 293T cells. LentiCRISPR v2 carrying sgRNA, pLV-EF1α-IRES-Blast-LINC08148, or pLV-EF1α-IRES-Blast-Src along with pSPAX2 (Addgene, 12260) and pVSVG (Addgene, 12259) were co-transfected into 293T cells using FuGENE HD Reagent (Promega). At 48 h, supernatants were passed through a 0.45-μm filter and were used for gene transduction.

To obtain bulk knockdown cells, cells were transduced with lentiviruses and were selected by puromycin (1 µg/mL) for about 1 wk. To select stable LINC08148^{KO} clones, cells were transferred to 10-cm dishes and were selected with 1 µg/mL of puromycin for 10–14 d to isolate single-cell clones.

To generate overexpression bulk cells, cells were transduced with lentivirus (pLV-EF1α-IRES-Blast-LINC08148 or pLV-EF1α-IRES-Blast-Src), followed by selection by Blasticidin (15 µg/mL) for 1 wk.

Gene silencing by siRNA

Sequence of siRNA targeting human *NRP1* was AACACCTAGTGGAGTGATA. Sequence of siRNA targeting human *SP1* was GCAACATGGGAATTATGAA. Control siRNA with scrambled sequence (siNC) was used as a negative control. siRNAs (16 nmol) were transfected into cells by using Lipofectamine 2000 Reagent (Invitrogen) according to the manufacturer's instructions. At 48 h post transfection, cells were harvested for further analysis.

Cytoplasm and nuclear RNA fraction assay

Cells were pelleted by centrifugation after washing three times with PBS. Cell pellets were treated with RLN buffer (50 mmol/L Tris-HCl, pH 8.0, 140 mmol/L NaCl, 1.5 mmol/L MgCl2, 0.5% [vol/vol] NP-40) on ice for 5 min to lyse plasma membrane. After centrifugation at 300 × *g* at 4°C, supernatants containing cytoplasmic extracts were transferred into new centrifuge tubes for RNA extraction by RNeasy Mini Kit (Qiagen, RY25, Germany), and the pellets were washed with RLT buffer (RNeasy Mini Kit) and were added with TRIzol reagent (Invitrogen) for RNA extraction.

CCK8 assay

Cell Counting Kit-8 (CCK8, MCE) reagent (80 µL) was added to cell culture (12-well plate) and was incubated at 37°C and 5% CO_2. After 1-h incubation, the OD value was measured at 450 nm using a BioTek Instrument (BioTek).

RNA-seq

Total RNAs of Ctrl and LINC08148^{KO} cells were extracted with TRIzol. Three biological replicates were performed. RNA quantification and integrity were measured by Agilent 4200 TapeStation. The libraries were sequenced on an Illumina PE150 platform. Differential expression analysis was performed using DESeq2 and DEXSeq. Enrichment of functions and signaling pathways analysis were performed based on GO and KEGG database.

RIP assay

293T cells were co-transfected with plasmids expressing LINC08148 together with pcDNA3.1(+) vector, SP1-HA, GRβ-HA, HNF1A-HA, or GTF2I-HA fusion proteins by Lipofectamine 2000 reagent (Invitrogen). At 24 h post transfection, the cells were lysed in RIP lysis buffer. Immunoprecipitation was carried out using anti-HA agarose (Sigma). Whole RNA extraction was performed using TRIzol reagent (Invitrogen) and was applied for qRT-PCR measurement.

Statistical analysis

All statistical analyses of viral RNA levels or viral titers were performed with an unpaired, two-tailed Student's *t*-test. Data were presented as mean ± standard deviation (SD).

ACKNOWLEDGMENTS

This work was supported by the National Natural Science Foundation of China (31970887, 82271385), Guangzhou Municipal Science and Technology Program (202206010114), and Natural Science Foundation of Guangdong Province (2022A1515010451). The funders had no role in the study design, data collection and analysis, decision to publish, or preparation of the manuscript.

AUTHOR AFFILIATIONS

[1]Key Laboratory of Tropical Diseases Control (Sun Yat-sen University), Ministry of Education, Guangzhou, China
[2]Department of Immunology and Microbiology, Zhongshan School of Medicine, Sun Yat-sen University, Guangzhou, China
[3]Department of Pathology, First Affiliated Hospital of Sun Yat-sen University, Guangzhou, China
[4]Food and Cosmetics Institute, Guangzhou Customs Technology Center, Guangzhou, China

AUTHOR ORCIDs

Chao Liu http://orcid.org/0000-0003-3863-7210
Ping Zhang http://orcid.org/0000-0002-5400-8767

FUNDING

Funder	Grant(s)	Author(s)
MOST | National Natural Science Foundation of China (NSFC)	31970887, 82271385	Ping Zhang
Guangzhou Municipal Science and Technology Bureau (GZST)	202206010114	Ping Zhang
GDSTC | Natural Science Foundation of Guangdong Province (廣東省自然科學基金)	2022A1515010451	Chao Liu

DATA AVAILABILITY

The RNA-seq data are available in the SRA database (BioProject ID: PRJNA949856).

ADDITIONAL FILES

The following material is available online.

Supplemental Material

Supplemental material (JVI01705-23-s0001.docx). Tables S1 to S4; Figures S1 to S6.

REFERENCES

1. Hayes EB. 2009. Zika virus outside Africa. Emerg Infect Dis 15:1347–1350. https://doi.org/10.3201/eid1509.090442
2. Weaver SC, Costa F, Garcia-Blanco MA, Ko AI, Ribeiro GS, Saade G, Shi PY, Vasilakis N. 2016. Zika virus: history, emergence, biology, and prospects for control. Antiviral Res 130:69–80. https://doi.org/10.1016/j.antiviral.2016.03.010
3. Teixeira FME, Pietrobon AJ, Oliveira L de M, Oliveira L da S, Sato MN. 2020. Maternal-fetal interplay in Zika virus infection and adverse perinatal outcomes. Front Immunol 11:175. https://doi.org/10.3389/fimmu.2020.00175
4. Runge-Ranzinger S, Morrison AC, Manrique-Saide P, Horstick O. 2019. Zika transmission patterns: a meta-review. Trop Med Int Health 24:523–529. https://doi.org/10.1111/tmi.13216
5. Parra B, Lizarazo J, Jiménez-Arango JA, Zea-Vera AF, González-Manrique G, Vargas J, Angarita JA, Zuñiga G, Lopez-Gonzalez R, Beltran CL, Rizcala KH, Morales MT, Pacheco O, Ospina ML, Kumar A, Cornblath DR, Muñoz LS, Osorio L, Barreras P, Pardo CA. 2016. Guillain-Barre syndrome associated with Zika virus infection in Colombia. N Engl J Med 375:1513–1523. https://doi.org/10.1056/NEJMoa1605564
6. Katz I, Gilburd B, Shovman O. 2019. Zika autoimmunity and Guillain-Barre syndrome. Curr Opin Rheumatol 31:484–487. https://doi.org/10.1097/BOR.0000000000000629
7. Parra MCP, Lorenz C, de Aguiar Milhim BHG, Dibo MR, Guirado MM, Chiaravalloti-Neto F, Nogueira ML. 2022. Detection of Zika RNA virus in *Aedes aegypti* and *Aedes albopictus* mosquitoes, Sao Paulo, Brazil. Infect Genet Evol 98:105226. https://doi.org/10.1016/j.meegid.2022.105226

8. Calle-Tobón A, Pérez-Pérez J, Rojo R, Rojas-Montoya W, Triana-Chavez O, Rúa-Uribe G, Gómez-Palacio A. 2020. Surveillance of Zika virus in field-caught *Aedes aegypti* and *Aedes albopictus* suggests important role of male mosquitoes in viral populations maintenance in Medellin, Colombia. Infect Genet Evol 85:104434. https://doi.org/10.1016/j.meegid.2020.104434
9. Musso D, Ko AI, Baud D. 2019. Zika virus infection - after the pandemic. N Engl J Med 381:1444–1457. https://doi.org/10.1056/NEJMra1808246
10. Hamel R, Dejarnac O, Wichit S, Ekchariyawat P, Neyret A, Luplertlop N, Perera-Lecoin M, Surasombatpattana P, Talignani L, Thomas F, Cao-Lormeau V-M, Choumet V, Briant L, Desprès P, Amara A, Yssel H, Missé D. 2015. Biology of Zika virus infection in human skin cells. J Virol 89:8880–8896. https://doi.org/10.1128/JVI.00354-15
11. Kaksonen M, Roux A. 2018. Mechanisms of clathrin-mediated endocytosis. Nat Rev Mol Cell Biol 19:313–326. https://doi.org/10.1038/nrm.2017.132
12. Xu MM, Wu B, Huang GG, Feng CL, Wang XH, Wang HY, Wu YW, Tang W. 2022. Hemin protects against Zika virus infection by disrupting virus-endosome fusion. Antiviral Res 203:105347. https://doi.org/10.1016/j.antiviral.2022.105347
13. Rinkenberger N, Schoggins JW. 2019. Comparative analysis of viral entry for Asian and African lineages of Zika virus. Virology 533:59–67. https://doi.org/10.1016/j.virol.2019.04.008
14. Owczarek K, Chykunova Y, Jassoy C, Maksym B, Rajfur Z, Pyrc K. 2019. Zika virus: mapping and reprogramming the entry. Cell Commun Signal 17:41. https://doi.org/10.1186/s12964-019-0349-z
15. Li M, Zhang D, Li C, Zheng Z, Fu M, Ni F, Liu Y, Du T, Wang H, Griffin GE, Zhang M, Hu Q. 2020. Characterization of Zika virus endocytic pathways in human glioblastoma cells. Front Microbiol 11:242. https://doi.org/10.3389/fmicb.2020.00242
16. Lee I, Bos S, Li G, Wang S, Gadea G, Desprès P, Zhao RY. 2018. Probing molecular insights into Zika virus(-)host interactions. Viruses 10:233. https://doi.org/10.3390/v10050233
17. Huang Y, Lin Q, Huo Z, Chen C, Zhou S, Ma X, Gao H, Lin Y, Li X, He J, Zhang P, Liu C. 2020. Inositol-requiring enzyme 1alpha promotes Zika virus infection through regulation of stearoyl coenzyme A desaturase 1-mediated lipid metabolism. J Virol 94:e01229-20. https://doi.org/10.1128/JVI.01229-20
18. Zhou S, Yang C, Zhao F, Huang Y, Lin Y, Huang C, Ma X, Du J, Wang Y, Long G, He J, Liu C, Zhang P. 2019. Double-stranded RNA deaminase ADAR1 promotes the Zika virus replication by inhibiting the activation of protein kinase PKR. J Biol Chem 294:18168–18180. https://doi.org/10.1074/jbc.RA119.009113
19. Liu S, DeLalio LJ, Isakson BE, Wang TT. 2016. AXL-mediated productive infection of human endothelial cells by Zika virus. Circ Res 119:1183–1189. https://doi.org/10.1161/CIRCRESAHA.116.309866
20. Zhang Y, Zhao S, Li Y, Feng F, Li M, Xue Y, Cui J, Xu T, Jin X, Jiu Y. 2022. Host cytoskeletal vimentin serves as a structural organizer and an RNA-binding protein regulator to facilitate Zika viral replication. Proc Natl Acad Sci U S A 119:e2113909119. https://doi.org/10.1073/pnas.2113909119
21. St Laurent G, Wahlestedt C, Kapranov P. 2015. The Landscape of long noncoding RNA classification. Trends Genet 31:239–251. https://doi.org/10.1016/j.tig.2015.03.007
22. Quinn JJ, Chang HY. 2016. Unique features of long non-coding RNA biogenesis and function. Nat Rev Genet 17:47–62. https://doi.org/10.1038/nrg.2015.10
23. Huang Z, Zhou JK, Peng Y, He W, Huang C. 2020. The role of long noncoding RNAs in hepatocellular carcinoma. Mol Cancer 19:77. https://doi.org/10.1186/s12943-020-01188-4
24. Li Y, Zhang H, Zhu B, Ashraf U, Chen Z, Xu Q, Zhou D, Zheng B, Song Y, Chen H, Ye J, Cao S. 2017. Microarray analysis identifies the potential role of long non-coding RNA in regulating neuroinflammation during Japanese encephalitis virus infection. Front Immunol 8:1237. https://doi.org/10.3389/fimmu.2017.01237
25. Bridges MC, Daulagala AC, Kourtidis A. 2021. LNCcation: lncRNA localization and function. J Cell Biol 220:e202009045. https://doi.org/10.1083/jcb.202009045
26. Zhu J, Fu H, Wu Y, Zheng X. 2013. Function of lncRNAs and approaches to lncRNA-protein interactions. Sci China Life Sci 56:876–885. https://doi.org/10.1007/s11427-013-4553-6
27. Kitabayashi J, Shirasaki T, Shimakami T, Nishiyama T, Welsch C, Funaki M, Murai K, Sumiyadorj A, Takatori H, Kitamura K, Kawaguchi K, Arai K, Yamashita T, Sakai Y, Yamashita T, Mizukoshi E, Honda M, Kaneko S, Hokuriku Liver Study Group. 2022. Upregulation of the long noncoding RNA HULC by hepatitis C virus and its regulation of viral replication. J Infect Dis 226:407–419. https://doi.org/10.1093/infdis/jiaa325
28. Robinson EK, Covarrubias S, Carpenter S. 2020. The how and why of lncRNA function: an innate immune perspective. Biochim Biophys Acta Gene Regul Mech 1863:194419. https://doi.org/10.1016/j.bbagrm.2019.194419
29. Winterling C, Koch M, Koeppel M, Garcia-Alcalde F, Karlas A, Meyer TF. 2014. Evidence for a crucial role of a host non-coding RNA in influenza A virus replication. RNA Biol 11:66–75. https://doi.org/10.4161/rna.27504
30. Lin H, Jiang M, Liu L, Yang Z, Ma Z, Liu S, Ma Y, Zhang L, Cao X. 2019. The long noncoding RNA Lnczc3h7a promotes a TRIM25-mediated RIG-I antiviral innate immune response. Nat Immunol 20:812–823. https://doi.org/10.1038/s41590-019-0379-0
31. Hu B, Huo Y, Yang L, Chen G, Luo M, Yang J, Zhou J. 2017. ZIKV infection effects changes in gene splicing, isoform composition and lncRNA expression in human neural progenitor cells. Virol J 14:217. https://doi.org/10.1186/s12985-017-0882-6
32. Azlan A, Obeidat SM, Theva Das K, Yunus MA, Azzam G. 2021. Genome-wide identification of *Aedes albopictus* long noncoding RNAs and their association with dengue and Zika virus infection. PLoS Negl Trop Dis 15:e0008351. https://doi.org/10.1371/journal.pntd.0008351
33. Wang Y, Huo Z, Lin Q, Lin Y, Chen C, Huang Y, Huang C, Zhang J, He J, Liu C, Zhang P. 2021. Positive feedback loop of long noncoding RNA OASL-IT1 and innate immune response restricts the replication of Zika virus in epithelial A549 cells. J Innate Immun 13:179–193. https://doi.org/10.1159/000513606
34. Seal RL, Chen L-L, Griffiths-Jones S, Lowe TM, Mathews MB, O'Reilly D, Pierce AJ, Stadler PF, Ulitsky I, Wolin SL, Bruford EA. 2020. A guide to naming human non-coding RNA genes. EMBO J 39:e103777. https://doi.org/10.15252/embj.2019103777
35. Tachiwana H, Saitoh N. 2021. Nuclear long non-coding RNAs as epigenetic regulators in cancer. Curr Med Chem 28:5098–5109. https://doi.org/10.2174/0929867328666210215114506
36. Cantuti-Castelvetri L, Ojha R, Pedro LD, Djannatian M, Franz J, Kuivanen S, van der Meer F, Kallio K, Kaya T, Anastasina M, et al. 2020. Neuropilin-1 facilitates SARS-CoV-2 cell entry and infectivity. Science 370:856–860. https://doi.org/10.1126/science.abd2985
37. Wang HB, Zhang H, Zhang JP, Li Y, Zhao B, Feng GK, Du Y, Xiong D, Zhong Q, Liu WL, Du HM, Li MZ, Huang WL, Tsao SW, Hutt-Fletcher L, Zeng YX, Kieff E, Zeng MS. 2015. Neuropilin 1 is an entry factor that promotes EBV infection of nasopharyngeal epithelial cells. Nat Commun 6:6240. https://doi.org/10.1038/ncomms7240
38. Carro SD, Cherry S. 2020. Beyond the surface: endocytosis of mosquito-borne flaviviruses. Viruses 13:13. https://doi.org/10.3390/v13010013
39. Benmerah A, Lamaze C. 2007. Clathrin-coated pits: vive la difference? Traffic 8:970–982. https://doi.org/10.1111/j.1600-0854.2007.00585.x
40. Mercer J, Schelhaas M, Helenius A. 2010. Virus entry by endocytosis. Annu Rev Biochem 79:803–833. https://doi.org/10.1146/annurev-biochem-060208-104626
41. Umasankar PK, Sanker S, Thieman JR, Chakraborty S, Wendland B, Tsang M, Traub LM. 2012. Distinct and separable activities of the endocytic clathrin-coat components Fcho1/2 and AP-2 in developmental patterning. Nat Cell Biol 14:488–501. https://doi.org/10.1038/ncb2473
42. Gottlieb-Abraham E, Shvartsman DE, Donaldson JC, Ehrlich M, Gutman O, Martin GS, Henis YI. 2013. Src-mediated caveolin-1 phosphorylation affects the targeting of active Src to specific membrane sites. Mol Biol Cell 24:3881–3895. https://doi.org/10.1091/mbc.E13-03-0163
43. Shajahan AN, Timblin BK, Sandoval R, Tiruppathi C, Malik AB, Minshall RD. 2004. Role of Src-induced dynamin-2 phosphorylation in caveolae-mediated endocytosis in endothelial cells. J Biol Chem 279:20392–20400. https://doi.org/10.1074/jbc.M308710200
44. Liu YG, Chen Y, Wang X, Zhao P, Zhu Y, Qi Z. 2020. Ezrin is essential for the entry of Japanese encephalitis virus into the human brain microvascular endothelial cells. Emerg Microbes Infect 9:1330–1341. https://doi.org/10.1080/22221751.2020.1757388
45. Pan W, Nie H, Wang H, He H. 2021. Bovine parainfluenza virus type 3 (BPIV3) enters HeLa cells via clathrin-mediated endocytosis in a

cholesterol- and dynamin-dependent manner. Viruses 13:1035. https://doi.org/10.3390/v13061035
46. Yuan M, Yan J, Xun J, Chen C, Zhang Y, Wang M, Chu W, Song Z, Hu Y, Zhang S, Zhang X. 2018. Enhanced human enterovirus 71 infection by endocytosis inhibitors reveals multiple entry pathways by enterovirus causing hand-foot-and-mouth diseases. Virol J 15:1. https://doi.org/10.1186/s12985-017-0913-3
47. Zhao R, Shi Q, Han Z, Fan Z, Ai H, Chen L, Li L, Liu T, Sun J, Liu S. 2021. Newcastle disease virus entry into chicken macrophages via a pH-dependent, dynamin and caveola-mediated endocytic pathway that requires Rab5. J Virol 95:e0228820. https://doi.org/10.1128/JVI.02288-20
48. Shamsul HM, Hasebe A, Iyori M, Ohtani M, Kiura K, Zhang D, Totsuka Y, Shibata K. 2010. The Toll-like receptor 2 (TLR2) ligand FSL-1 is internalized via the clathrin-dependent endocytic pathway triggered by CD14 and CD36 but not by TLR2. Immunology 130:262–272. https://doi.org/10.1111/j.1365-2567.2009.03232.x
49. Ritchie S, Boyd FM, Wong J, Bonham K. 2000. Transcription of the human c-Src promoter is dependent on Sp1, a novel pyrimidine binding factor SPy, and can be inhibited by triplex-forming oligonucleotides. J Biol Chem 275:847–854. https://doi.org/10.1074/jbc.275.2.847
50. Bonham K, Ritchie SA, Dehm SM, Snyder K, Boyd FM. 2000. An alternative, human SRC promoter and its regulation by hepatic nuclear factor-1alpha. J Biol Chem 275:37604–37611. https://doi.org/10.1074/jbc.M004882200
51. Miyamoto N, Higuchi Y, Tsurudome M, Ito M, Nishio M, Kawano M, Sudo A, Kato K, Uchida A, Ito Y. 2000. Induction of c-Src in human blood monocytes by anti-CD98/FRP-1 mAb in an Sp1-dependent fashion. Cell Immunol 204:105–113. https://doi.org/10.1006/cimm.2000.1696
52. Gammie AE, Kurihara LJ, Vallee RB, Rose MD. 1995. DNM1, a dynamin-related gene, participates in endosomal trafficking in yeast. J Cell Biol 130:553–566. https://doi.org/10.1083/jcb.130.3.553
53. Russell T, Samolej J, Hollinshead M, Smith GL, Kite J, Elliott G. 2021. Novel role for ESCRT-III component CHMP4C in the integrity of the endocytic network utilized for herpes simplex virus envelopment. mBio 12:e02183-20. https://doi.org/10.1128/mBio.02183-20
54. McMahon HT, Boucrot E. 2011. Molecular mechanism and physiological functions of clathrin-mediated endocytosis. Nat Rev Mol Cell Biol 12:517–533. https://doi.org/10.1038/nrm3151
55. Mettlen M, Chen PH, Srinivasan S, Danuser G, Schmid SL. 2018. Regulation of clathrin-mediated endocytosis. Annu Rev Biochem 87:871–896. https://doi.org/10.1146/annurev-biochem-062917-012644
56. Chu JJH, Yang PL. 2007. c-Src protein kinase inhibitors block assembly and maturation of dengue virus. Proc Natl Acad Sci U S A 104:3520–3525. https://doi.org/10.1073/pnas.0611681104
57. Chen JH, Feng DD, Chen YF, Yang CX, Juan CX, Cao Q, Chen X, Liu S, Zhou GP. 2020. Long non-coding RNA MALAT1 targeting STING transcription promotes bronchopulmonary dysplasia through regulation of CREB. J Cell Mol Med 24:10478–10492. https://doi.org/10.1111/jcmm.15661